AD-A162 712 SPECTRAL DIVERSITY CRYSTALLINE FLUORIDE LASERS(U) 1/1
MASSACHUSETTS INST OF TECH CAMBRIDGE
H P JENSSEN ET AL. 1981 N00014-81-K-0476

UNCLASSIFIED F/G 20/5 NL

END
FILMED
DTIC

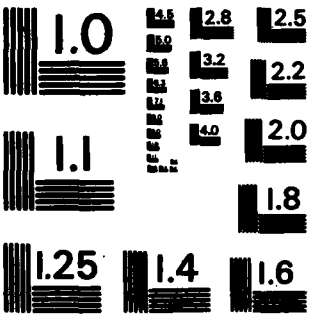

MICROCOPY RESOLUTION TEST CHART
NATIONAL BUREAU OF STANDARDS-1963-A

SPECTRAL DIVERSITY CRYSTALLINE FLUORIDE LASERS

H. P. Jenssen, D. R. Gabbe, A. Linz, & C. S. Naiman
Crystal Physics and Optical Electronics Laboratory
Center for Materials Science and Engineering*
Massachusetts Institute of Technology
Cambridge, Massachusetts 02139

Micrometers

Abstract

Within the realm of crystalline laser materials, the class of fluorides distinguishes itself mostly by the wide variety of laser wavelengths displayed. Laser operation has now been reported from 3.9 μm in the infrared to 286 nm in the ultraviolet. Many are operated flash-lamp pumped, while others have shown high utility as linear down conversion lasers and are pumped by other laser sources. Some operate with essentially one primary ion, usually a rare earth ion, while others are sensitized by other co-dopants which absorb the pump energy and transfer it to the active laser ions. The potential of large spectral diversity for laser operation is due both to the wide window of transparency that fluorides possess and the lower rates of non-radiative decay. The high band gap in the ultraviolet also leads to low linear absorption, low non-linear refractive indices and multiphoton absorption. Additionally, the good chemical stability displayed by high purity stoichiometric fluoride compounds allows their use with ultraviolet pump sources at high energies, without incurring UV induced damage. We review the most recent research associated with such materials, particularly the host crystal, lithium yttrium fluoride, $LiYF_4$ (YLF).

1.0 Introduction

Within the realm of crystalline laser materials, the class of fluorides distinguishes itself mostly by the wide variety of laser wavelengths displayed. Laser operation has now been reported from 3.9 μm, in the infrared,[1] to 286 nm in the ultraviolet[2]. Many are operated flash-lamp pumped, while others have shown high utility as Linear Down Conversion Lasers[3] (LDCL) and are pumped by other laser sources. Some operate with essentially one primary ion, usually a rare earth ion, while others are sensitized by other co-dopants which absorb the pump energy and transfer it to the active laser ions.

The potential of large spectral diversity for laser operation is due to the wide window of transparency that fluorides possess. The ability to sustain laser operation between a given set of energy levels in fluorides is enhanced over oxides because of the lower rates of non radiative decay.

The high band gap in the ultraviolet not only leads to low linear absorption, but also to low non-linear refractive indices[4] and multiphoton absorption.[5] Additionally, the good chemical stability displayed by high purity stoichiometric fluoride compounds allows their use with ultraviolet pump sources without incurring UV induced damage.

The same phonon properties that lower non-radiative decay lead to thermal and mechanical properties of fluorides that are not as good as oxides. However they are superior in these same properties with respect to glasses.

In this review of the most recent research associated with such materials, we will focus mostly, though not exclusively, on the host crystal, lithium yttrium fluoride, $LiYF_4$ - often shortened as YLF. Tables I and II show the mechanical, thermal, and optical properties of this host material.

In the following sections we will discuss some of the characteristics of the various RE^{+3} ($4f^n$) lasers, usually flash pumped. The important case of the cw operation with Nd:YLF will also be described. We then will discuss linear down conversion lasers with the cases Ho:YLF and Er:YLF pumped by 532 nm and of Tm:YLF resonantly pumped by the XeF laser. Sensitization by other ions is exemplified by the Ho:αβYLF laser, and some of its tunable properties will be mentioned.

Figure 1 displays the energy level diagram of the rare earth ions we will be discussing. Table III lists the energy levels and the laser wavelengths, shown as arrows in Figure 1.

2.0 Cerium (Ce^{+3}-$4f^1$)

Cerium has operated as a laser in two fluoride hosts - YLF at 325 nm[6] and in LaF_3 at 286 nm[2]. Ce:YLF is tunable at 325 nm and 309 nm.[7]

Ce^{+3} is a rare earth ion with the $4f^1$ configuration and the laser transitions in this ion are between the $4f^0\ 5d^1$ and the $4f^1$ states. The upper pump levels are 5d states that are split by the crystal field and pumping in these materials has been accomplished by a KrF excimer-laser operating at 249 nm. The upper laser level undergoes a large Stokes shift between emission and absorption, of approximately 2,000 cm^{-1}. This appears to assist in four level operation by circumventing the potential bottleneck in the lower laser level ($^2F_{7/2}$), which has a lifetime of approximately 10 microseconds.

The vibronic nature of the fluorescence from the $4f^0\ 5d^1$ states has also been utilized to advantage. Erlich et al.[7], have recently achieved tunable operation of the Ce doped YLF

*Work supported by various contracts with ONR, AFOSR, AFAL, DOE, NSF, DARPA, ECOM, and NVOEL (through the Center for Materials Science and Engineering).

crystal in two bands between 305 to 306 nm, and 323 to 328 nm. In oxides, Ce^{+3} has not operated as a laser, presumably because of Excited State Absorption (ESA). Such ESA does not appear in fluorides. This is not well understood and may be because of the different crystal field strengths.

3.0 Praseodymium (Pr^{+3} - $4f^2$)

L. Esterowitz, et al.,[8] have reported laser operation in the blue for 0.2% doped Pr:YLF. Lasing was accomplished at room temperature by pumping with a tunable flash lamp-pumped dye laser at 444 nm exciting the Pr ion from the $^3H_4$ ground state to the $^3P_2$ excited state. The excited ion then decays to the lowest of these excited states, the $^3P_0$ state, and lasing action proceeds between it and the lowest level of the group manifold at 479 nm. They also attempted laser action to the other levels of the $^3H_4$ ground manifold, 493 cm^{-1} and 83 cm^{-1} above the ground level. With a lower thermal population, these levels should produce inversion more easily, but their cross sections are sufficiently weaker so that the three level laser action to lowest state is all that is seen.

Morrison et al.[9] have studied the potential of using other fluoride hosts such as KY_3F_{10} as a suitable matrix for Pr, so that it would operate as a more nearly four level laser. Their calculations suggest that operation at 77°K may allow four level action.

Pumping the excited states of the Pr ion is difficult because the absorption is so narrow, forcing one to use a "resonant" laser pump. It might be possible to make use of other ions that couple better to other pumps, that would then sensitize the Pr ion. This could be through the $^1S_0$ higher lying state in the region of 50,000 cm^{-1}, or the states around 21-22,000 cm^{-1}. Ce^{+3} shows some potential for this, but in most fluorides the cerium fluorescence tends to fall in the 300-350 nm region, just where Pr has a window.

4.0 Neodymium (Nd^{+3} - $4f^3$)

Results on Nd laser operation, in any materials, including fluorides, deserve comparison to the "workhorse" of Nd lasers, namely Nd:YAG. One aspect of the importance of Nd:YLF lies in the dual wavelength of operation 1.053 and 1.047 μm, corresponding to its σ and π polarizations[10,11]. Since Nd:YAG operates at 1.064 μm, the 1.053 μm Nd:YLF line is a much better match to fluorophosphate and phosphate glasses that operate at 1.054 μm. Additionally, the Nd:YLF line at 1.047 μm is a better match to fluoroberylate and other fluoride glasses[12]. Such materials are used in Inertial Confinement Fusion (ICF) applications[13,14,15] and Nd:YLF serves as the oscillator in such systems.

Such ICF applications utilize short pulses. Le Goeff et al.[12] have found, in data taken in the same cavity on Nd:YLF and Nd:YAG, that pulsewidths from the two are comparable. Pumping with approximately 40 joules, they achieved outputs of 8 millijoules from Nd:YLF in a TEM_{00} mode with a pulsewidth of 35 ± 5 picoseconds. However, in their measurements the energy stability in Nd:YLF appears better than YAG. They attribute this to the much longer lifetime in YLF of 500 microseconds vs. 240 microseconds for Nd:YAG.

It has been found in continuous operation, that in comparison to Nd:YAG, Nd:YLF exhibits a lower threshold and higher single mode average power.[16] The mode volume of Nd:YLF was observed to be a factor of four larger than Nd:YAG resulting in twice the TEM_{00} mode average power. This result is due to the substantially lower thermal lensing in YLF with respect to YAG because of a negative dn/dt in YLF[17]. We provide in Table IV the thermal properties of Nd:YLF compared to Nd:YAG and Nd:Glass.

In the process of carrying out the above work, the stimulated emission cross section was also measured for both Nd:YLF and Nd:YAG. Using the Einstein relations, assuming unit quantum efficiency, it is possible to get accurate relative values without the need for determination of the active ion density. Figure 2 gives these data for the 1.03 μm to 1.13 μm region. Table V lists the values at the 3 laser wavelengths.

The lower cw threshold is attributed to the fact that the product of the emission cross section of the laser transition and its lifetime is larger by approximately 1.5 for YLF vs. YAG. The slope efficiency, however, was lower for Nd:YLF and this is not understood.

The combination of lower distortion under high power conditions and longer lifetime, gives this material a potentially much higher advantage with respect to YAG in lasers using high repetition rate Q-switch operation. For a material with lifetime τ, operating at a frequency repetition rate of f, one can show that for low repetition rates ($\tau \times f << 1$), the average power $P_{av} = P_{cw} \tau f$. Here P_{cw} is the cw power. P_{av} in Nd:YLF can be predicted to be as much as a factor of two above that for Nd:YAG. Similarly, the longer lifetime allows for storage of more energy per pulse and for a higher peak power, even up to rates of 5kHz. Since it is linearly polarized, all of the above become valuable attributes in e-o Q switching and doubling to the 500 nm region.

5.0 Terbium (Tb^{+3} - $4f^8$)

Tb:YLF has operated as a laser at 544.4 nm from the $^5D_4$ to the $^7F_5$ transition.[18] However, as a four level laser in the green, it appears to be inefficient due to a low stimulated emission cross section and pump bands that are at 26,000 cm^{-1} and above. Spectroscopic measurements of $LiTbF_4$ were carried out at room and liquid nitrogen temperatures.[19] The stimulated emission cross section for the 545 nm $LiTbF_4$ transition were 1.5×10^{-21} cm^2 at 77°K and 1.0×10^{-21} cm^2 at room temperature. At room temperature the 545 nm transition requires a 50 joule/inch flashlamp input threshold for 25% Tb doped YLF.

It has also been evaluated as a potential material for LDCL operation with rare gas halide pumping, but this also does not appear to be very fruitful.[3]

More uses of crystalline fluorides doped with this ion appear to lie in their magneto-optical properties. M. J. Weber et al.[20] have studied the Faraday rotation of crystals of KTb_3F_{10}, $LiTbF_4$, $LiTb_{0.5}Y_{0.5}F_4$, and $LiTb_{0.25}Gd_{0.75}F_4$ with respect to wavelength, temperature and magnetic field dependence. Devices based on the Faraday effect include optical rotators, isolators, modulators and high voltage sensors. For these applications, a large Verdet constant, small absorption and scattering losses, and, in high power lasers, a small linear refractive index and non-linear refractive index are important properties. Some form of isolators must be utilized to control timing and direction of the laser pulse between stages in the amplifier chain in high power laser amplifiers.

The Verdet constants of two of these crystals are given in Table VI. The importance of such materials lies in not only having a large Verdet constant (other materials such as terbium garnets have even greater values), but rather in combining such large values with the low linear and nonlinear refractive indices of such materials. Thus, the estimated value for terbium garnet is 8.6×10^{-20} m^2/watt, and comparatively for terbium doped glasses, is 5.3×10^{-20} m^2/watt measured for FR-5 glass.

However, it is most important to include self-focusing, since this is a basic limitation with the very high peak power lasers as in Inertial Confinement Fusion applications. A proper figure of merit is then the linear index, times the Verdet constant, divided by non-linear coefficient. Based on these results KTb_3F_{10} and $LiTbF_4$ are superior to both garnet crystals and glasses. Table VI includes such a figure of merit along with other optical properties of KTb_3F_{10} and $LiTb_4$, compared to FR-5 glass.

6.0 Holmium (Ho^{+3} - $4f^{10}$)

As can be seen from Figure 1, holmium and the ion that we will discuss in the next section, erbium, have displayed the greatest number of laser transitions. It can be seen from their energy level diagrams that both in Ho and Er spacings of 2-3-4,000 cm^{-1} between adjacent states are common in these ions. In oxides, multi-phonon effects generally quench fluorescence for such energy level splittings. By contrast, in fluorides (and certainly for heavier ions such as chlorides) fluorescence is not quenched, allowing for the potential of laser operation.

E. P. Chicklis et al. have reported in 1971 the efficient room temperature operation of Er, Tm sensitized Ho:YLF operating at 2.06 μm[21]. In comparative studies with YAG as a host, it was found to have greater efficiency, and be less susceptible to laser induced damage.[22] This sensitized operation at 2.06 μm stimulated considerable research into YLF as a host, and it led to the availability of the material. This, in turn, stimulated experiments at other wavelengths.

Efficient operation of Ho in co-doped Tm^{+3}, Er^{+3} hosts, goes back to the early days of laser operation when it was first accomplished in YAG.[23] These are often referred to as αβHo: lasers [21]. Such lasers, both in cw and in pulsed operation, are very efficient because of their strong absorption of pump light and, in some cases, quantum efficiencies greater than 1 have been seen[23] for the sensitization process.

The efficient sensitization of Ho^{+3} at 2.06 μm by codoping with Er^{+3} and Tm^{+3} can be appreciated from the energy level diagram, Fig. 3. Quantum efficiencies of 3 have been observed consistent with the following energy level decays:

(a) An excited Er^{+3} ion from the $^4S_{3/2}$ state decays to the $^4I_{9/2}$ state, simultaneously bringing a Tm^{+3} ion from its ground $^3H_6$ state up the $^3H_4$ excited state;

(b) Next the Er^{+3} excited ion in the $^4I_{9/2}$ state decays to the $^4I_{13/2}$ state in Er^{+3}, simultaneously exciting a second Tm^{+3} ion from its $^3H_6$ ground state to the $^3H_4$ upper state; and then

(c) The excited Er^{+3} ion in the $^4I_{13/2}$ state decays to the $^4I_{15/2}$ Er^{+3} state, simultaneously exciting a third Tm^{+3} ion from the $^3H_6$ ground state up to the $^3H_4$ excited state. Thus one excited Er^{+3} ion (in the green) can yield three excited Tm^{+3} ions, which can now transfer to the Ho^{+3} $^5I_7$ states.

(Parenthetically we should note that the $^4F_{9/2}$ excited Er^{+3} ion can also transfer over to the $^3F_2$ excited state of Tm^{+3} decaying down to the Tm^{+3} $^3F_4$ state. From $^3F_4$ it will deay down to the $^3H_4$ state, simultaneously exciting an additional Tm^{+3} ion from its ground state $^3H_6$ to $^3H_4$, while leaving the other excited ion in its upper state, giving two excited Tm^{+3} ions. This corresponds to a quantum efficiency of two.) A fraction of the Tm^{+3} ions in the $^3H_4$ state transfer over to Ho^{+3} in the upper $^5I_7$ state, being able then to participate in laser operation. This fraction is temperature dependent since these two sets of levels appear to thermalize. This fact, as well as the presence of competing upconversion processes which tend to deplete the populations of both the sensitizing and laser levels, limit the overall efficiency of the αβHo:YLF laser, although it still compares favorably with Nd:YAG.

Barnes et al.[28] have reported on low temperature operation (ca. 80°K) of an αβHo:YLF laser in a TEM_{00} Q-switched mode with up to 150 mj per pulse. While complete analysis of this complex material is difficult, cooling to 80°K gives a much lower threshold by increasing the relative population of the upper laser level and giving quasi-four level operation since the terminal level is 300 cm^{-1} above the ground state.

A. M. Morozev, et al.(24) and Podkolzinia et al.[25] have reported numerous laser transitions in $LiHoF_4$ and 2% Ho:YLF at low temperatures including the $^5S_2 \rightarrow {}^5I_7$ transition in the

750 nm region. These are listed in Table III. E. P. Chicklis, et al.[26] have reported laser operation of this transition in 2% Ho:YLF at room temperature. They utilized both flashlamp and dye laser pumps as the excitation mechanism. Thresholds of 4 joules/cm and 3×10^{-4} joules/cm were observed in flashlamp and dye laser pumped operation respectively. The stimulated emission cross section of $\sigma = 9.7 \times 10^{-19}$ cm^2 was measured with an upper level lifetime of 90 ± 10 microseconds, and a lower level lifetime of ~15 milliseconds at room temperature. Performance limitations imposed by the long lower manifold lifetime can be overcome by co-doping with other rare earth ions, as long as the upper state is not also quenched. More recently it has been found that there is a very weak absorption in Ho:YLF at 750 nm which limits its potential utilization at this wavelength. This will be discussed in section 8.0 in connection with linear down conversion lasers. Operation down to 4.2°K has allowed laser oscillation at 1153 nm, 889.7 nm, 645.4 nm, and 540.8 nm, corresponding to transitions from the $^5I_6$, $^5I_5$ $^5F_5$, and $^5S_2$ upper laser levels to the ground $^5I_8$ state.

The energy level structure of Ho:YLF also lends itself to operation as a cascade laser.[24] This has led to the longest wavelength room temperature operation in solid state crystalline fluoride lasers, namely at 3.914 μm.[1]

Two cascade laser schemes were demonstrated in this material. The first involved the triad of states $^5S_2 \rightarrow {}^5I_5 \rightarrow {}^5I_7$ levels, and led to the laser oscillation at 1.392 and 1.673 μm. The second included the triad $^5S_2 \rightarrow {}^5I_5 \rightarrow {}^5I_6$ levels leading to oscillations at 1.392 and 3.914 μm. The pump in the work by Esterowitz et al.[1] was the doubled output of a Nd:Glass (ND-2) laser operating at 535 nm, matched to the absorption peak of the $^5F_4$ level of the Ho:YLF material.

Ho:YLF and $LiHoF_4$ are lasers which have operated at 979 nm at room and low temperatures[24] respectively. Because double this wavelength, at 490 nm, provides operation in the blue/green, this has been investigated for potential operation at or near room temperature. At 300°K, the cross section and lifetime of the $^5F_5$ level were measured to be 4×10^{-20} cm^2 and 16 microseconds respectively. The lower laser level, $^5I_7$, has a lifetime of 15 milliseconds which could become a bottleneck. The short upper state lifetime is significant since a flash lamp pump source will need to be ultra-fast in order to achieve efficient laser operation.[29]

The Ho^{+3} $^5I_6$ level has the interesting property that it appears to maintain a long fluorescent lifetime even in the presence of large amounts of Ho^{+3} and/or Er^{+3}. Because of this, it lases at 2.9 μm with a very low threshold at room temperature.[30]

Because of its wavelength of operation, 2.06 μm, αβHo:YLF has been considered for eye safe laser systems operating through the atmosphere.[31] It has been reported by White et al.[32] that the absorption in the $4\nu_2 + \nu_3$ combination band of atmospheric CO_2 is great enough to cause considerable attenuation of the beam even over a shortened path length, because the laser radiation is coincident with one of the absorption lines.

Because it may be important to control the wavelength output of the laser, Erbil and Jenssen[33] have carried out a study of the tunability of the Ho:YLF laser around 2.06 μm. Tuning was carried out by a number of techniques, with the best results utilizing a mirror/grating combination. Figure 4 shows the relative power output for this laser in the 2.0610 to 2.0660 μm region. The fluorescence intensity output associated with the two polarizations is shown in Figure 5. Figure 6 gives the stimulated emission cross-section at room temperature for the two polarizations.

In order to confirm that the multiple wavelengths emitting from the laser would "get around" the CO_2 laser absorption, atmospheric transmission measurements were carried out over a distance of twelve kilometers. The experiments were performed in clear weather with visibility greater than 16 kilometers (10 miles). The total attenuation of the received signal was very similar to propagation experiments performed with a frequency doubled Nd:YAG laser at 532 nm. While the output wavelength was tuned over the region indicated in Figure 4, the received signal was monitored to detect any deep fading associated with the CO_2 absorption. No such fading was observed probably because stepwise change in output missed the lines. In any event, it appears that atmospheric applications would not be seriously affected.

7.0 Erbium (Er^{+3} - $4f^{11}$)

As mentioned earlier, Er shares a lot of similarity with Ho, and many of the comments previously mentioned in Section 6.0 apply to Er. First, it, too, has a three-level, laser transition from its long lived lowest excited state, $^4I_{13/2}$, to the ground state, $^4I_{15/2}$, at 1.6 μm. This state can be sensitized by other ions such as Yb^{+3}. Extensive work has been done in glasses co-doped this way, which are then pumped by the 1.06 μm radiation of a Nd laser.[34] Such materials also share the motivation of the 2.06 μm $^5I_7 \rightarrow {}^5I_8$ Ho:αβYLF transition, namely to render laser equipment eye safe.

In this context, another transition in Er:YLF has greater systems potential, because it is a 4-level rather than 3-level laser. Figure 7 gives the energy level diagram of Er^{+3} with the $^4S_{3/2}$ to $^4I_{9/2}$ laser line shown by the arrow. This operates at 1.73 μm and has many of the advantages[2] (identified on the figure) that are lacking in other competive materials. It is a true four-level transition; it rapidly relaxes to the upper laser level $^4S_{3/2}$; it has no ground state absorption or excited state absorption at 1.73 μm and has a long upper level lifetime, allowing for convenient flash pumped operation.

Reference (35) discusses Er:YLF laser operation at 850 nm, 1.22 μm, and 1.74 μm under flash pumped operation. M. Knights et al.[36] have achieved 30 millijoule output in Q-switched single pulses from a 5 x 60 mm rod with approximately 28 lamp joules input. (See

Figure 7.) Working with a transmitted energy of 10 millijoules for ranges of 0.5 kilometers, they were able to achieve a signal-to-noise ratio of 1000:1 using a G.E. photo diode detector against man-made targets. It appears that 20 millijoules should be useful for rangefinding up to 5 kilometers using a 3" aperture receiver with a signal-to-noise ratio of 10. Such a system appears to compete effectively with CO_2 rangefinders in terms of penetrability through smoke.

Multifrequency cascade emission has been seen in Er^{+3} similar to Ho^{+3}(37) as shown in the energy level diagrams and listings, Figure 1 and Table III respectively. Again, similar to the case of the Ho^{+3} $^5I_6$ level, the Er^{+3} $^4I_{11/2}$ level appears to retain its lifetime even in the presence of other ions such as Ho^{+3} and Er^{+3}. Thus, laser transitions that originate from that level appear to be achievable even with high doping of Ho^{+3} and Er^{+3} that help absorb the pump light radiation, and at room temperature.

Reference (37) also describes cascade operation corresponding to the triad, $^4S_{3/2} \rightarrow {}^4I_{11/2} \rightarrow {}^4I_{13/2}$ with operation at 1.23 μm and 2.87 μm respectively. Another cascade scheme, using four levels, which leads to two laser wavelengths, corresponds to $^4S_{3/2} \rightarrow {}^4I_{9/2}$ with laser operation at 1.72 μm, then rapid decay to the $^4I_{11/2}$ state, and a laser transition from $^4I_{11/2}$ to $^4I_{13/2}$ at 2.87 μm. Petrov and Tkachuk (37) also recommend other rare earth ions for co-doping, in order to speed up relaxation from the $^4I_{13/2}$ to the ground state, so that it does not become a bottleneck. Of these, the best is the Tb^{+3} ion which has no energy levels that would interfere with the Er^{+3} ion from 7,000 cm^{-1} to 20,000 cm^{-1}, and thus does not quench any of the upper energy levels of the Er^{+3} ion. Such co-doping to speed up the transition from the $^4I_{13/2}$ state has been reported by Chicklis et al.(35)

L. Esterowitz et al.(38) have carried the cascade laser scheme further, projecting for an Er:YLF crystal the ability to operate at wavelengths spanning the visible to mid-IR spectral regions. These would include 540 nm corresponding to the 3-level operation of $^4S_{3/2}$ to the $^4I_{15/2}$ ground state transition. Additionally, the following cascade $^4S_{3/2} \rightarrow {}^4F_{9/2} \rightarrow {}^4I_{9/2} \rightarrow {}^4I_{11/2} \rightarrow {}^4I_{13/2}$ is projected, corresponding to laser emission at 3.3 μm, 3.8 μm, 4.8 μm, and 2.8 μm. (To date the first three have not been observed.)

To further improve the ability to create laser action, it is possible to Q-switch the laser transition that feeds the upper energy level of the desired laser transition. This greatly increases the pumping speed and overcomes energy level depopulation due to non-radiative relaxation. Esterowitz et al.(38) also suggest that cooling to low temperatures may be desirable.

Er^{+3} and Ho^{+3} have been combined in a single crystal of YLF and laser operation has been achieved at two colors in the same crystal. The wavelengths were 750 nm with Ho^{+3} and 850 nm with Er^{+3}(39). The upper laser levels of both ions are coupled together with reversible energy transfer, and each one "sensitizes" the other. Thus in this laser, we are able to see both sensitization, whereby each ion sensitizes the other, and also wavelength diversity, by combining multiple active laser ions in one host.

Simultaneous operation of laser transitions from Nd^{+3} and Yb^{+3} in a glass host had been reported in the early days of laser operation but without evidence of cosensitization.(40) Figure 8 shows the energy levels involved for the Ho^{+3} and Er^{+3} ions. It will be noted that the two upper laser levels, namely $^5S_2$:Ho^{+3}, and $^4S_{3/2}$:Er^{+3} are virtually coincident, and have relatively long lifetimes. Thus they have the opportunity to sensitize each other, and Chicklis et al.(39) have carried out an analysis of such self sensitization.

Both cw and pulsed selective excitation were used to measure the various rates. Figure 9 shows the Ho^{+3} and Er^{+3} emission spectra under selective excitation by an argon laser. It was found that the transfer efficiency is higher going from Er^{+3} to Ho^{+3} than the reverse, due to the longer fluorescent lifetime of the Er^{+3} $^4S_{3/2}$ level.

Because of some accidental degeneracies, it is possible to have considerable transfer and quenching back and forth between the different ions. These are suggested in Figure 10. In addition there are also other competitive rates of self-quenching in Er^{+3} and Ho^{+3} which are the kind that are observed in singly doped crystals.

Pulsed laser measurements were carried out using a rod of 3.5% Er^{+3} - 2% Ho^{+3} of dimensions 5 x 50 mm. The rod was high reflectivity coated at 750 to 850 nm at one end, and anti-reflection coated at the other end. Single operation of 850 nm only, and simultaneous operation of 750 and 850 nm are shown in Figure 11. The measurements showed that the predominant power output for the choice of concentrations is at 850 nm, in the Er^{+3} ion. The threshold at 750 nm is a factor of 5 higher than the 850 nm threshold. During simultaneous laser operation it was noted that the Ho^{+3} laser output "turned off" even before the pump pulse reached its maximum, whereas the Er^{+3} output followed the pump pulse shape. There was, however, some delayed output of the Er^{+3} emission, up to 100 microseconds after the pump pulse. Both these effects might be due to population buildup in lower levels causing excited state absorption. Such transitions, however, were not identified.

Laser measurements at room temperature in the same crystal and in a more efficient laser cavity were also carried out. In these tests only the 850 nm oscillations were observed, and no 750 nm oscillations were detected at up to three times the 850 nm threshold. This may have been an artifact of the experimental conditions, based on flashlamp pulse width, etc. It was conjectured that different concentrations of the rare earth ions and/or in different hosts may lead to more nearly optimum multi-ion performance.

8.0 Linear Downconversion Lasers (LDCL)

Spectral diversity in laser materials may be greatly extended through laser pumping that "shifts" the laser energy downward. As opposed to non-linear parametric oscillators, this is a linear process. Furthermore, low heat loading with high efficiency appears obtainable by resonantly pumping the upper laser level of a solid, in which the laser output is near the pump frequency, and in which the predominant mode of all subsequent relaxations is radiative. Fluorides again have the advantage over oxides because of their lower nonradiative relaxation rates given a fixed energy level band gap.

This is conceptualized in Figure 12, as the "Ideal Resonantly Pumped Laser." Further requirements include a metastable lifetime that exceeds the pump duration and a host material in which the damage resistance exceeds the pump fluence for high performance operation (high peak and high average powers). Since laser pulses can be engineered to be ultrashort, even levels with very short metastable lifetimes in the LDCL material can be made to operate as a laser. Other advantages of the process of linear down conversion in solids are shown in Table VII.

Table VIII provides a convenient listing of resonantly pumped crystalline lasers. Whereas a variety of laser pumps have been utilized, all of the host materials are fluorides. In addition to the host crystal of YLF, MgF_2 doped with the transition metal ions Ni^{2+} and Co^{2+}, have been laser pumped by P. Moulton[41] and operated as tunable lasers in the infrared region.

An important case of such a LDCL is shown in Figure 13. M. G. Knights et al.[42] have reported on frequency conversion of doubled Nd:YAG operating at 532 nm in both Ho:YLF and Er:YLF. By resonantly pumping the laser transitions in the solid medium, conversion efficiencies of up to 25% were demonstrated, at pump limited repetition rates of up to 40 hz.

Frequency doubled Nd:YAG laser systems are a convenient laser pump because considerable numbers of high performance (high peak and average power) systems based on 532 nm are finding their way into current usage. Ordinarily, this laser wavelength is used to pump organic dye lasers in order to fill in the wavelength region between 532 and 1064 nm. However, it is difficult to achieve efficient dye operation at wavelengths beyond 700 nm. Additionally, dye systems require complex designs to overcome thermally induced distortion at high average power loading. Also, because of their chemical nature, photo-induced instabilities often degrade the lifetime of the organic dye solutions. By contrast, the use of rare earth doped solids would appear to be extremely attractive because of their chemical stability, and the fact that thermal properties of solids are far superior to liquids. Perhaps most important though, and closely related to the major theme of this paper, is the importance of being able to provide wavelength shifts well into the infrared, where dyes do not operate at all.

Fortuitously, both Ho^{+3} and Er^{+3} in YLF, exhibit absorption in the 532 nm region by a metastable level from which a variety of laser transitions have previously operated. In Ho:YLF, the $^5F_4$ manifold is populated by the 532 nm pump. This is followed by rapid multi-phonon relaxation to the lowest level of the $^5S_2$ manifold, which serves as the upper laser level for the 750 nm laser transition, $^5S_2 \rightarrow {}^5I_7$.

In Er:YLF, the 532 nm pump populates the $^4S_{3/2}$ state via the $^2H_{11/2}$ state. The lowest level of this manifold serves as the upper laser level for the 850 nm laser transition, $^4S_{3/2} \rightarrow {}^4I_{13/2}$. In both cases the terminal laser level is long lived and decays radiatively to the ground state, thus not burdening the crystal with a thermal decay.

Figure 14 shows the data associated with the resonantly pumped Er:YLF laser similar to Figure 13 for the Ho:YLF laser.

The frequency doubled Nd:YAG laser used in these experiments provided a multi-mode Q-switched pulse of up to 20 millijoules at 532 nm with a pulse width of approximately 20 nanoseconds. The Ho:YLF/Er:YLF crystals were pumped longitudinally, the pump beam passing through a focusing lens and one laser mirror. This mirror was coated for maximum reflectivity at 750/850 nm with approximately 90% transmission at the pump wavelength. Short radius-of-curvature mirrors and a confocal resonator geometry were employed to ease potential alignment difficults.

Using coupling mirror reflectivities of 65% for Ho:YLF and 85% for Er:YLF, conversion efficiencies (defined as the ratio of absorbed pump energy to output energy) of 19.8% and 28.9% respectively were obtained. In both cases the pulse repetition rate was varied from 1 to 40 hz with no measurable reduction in conversion efficiency. Sustained operation was limited by the duty cycle of the pump laser, but the system was run at 15 hz for a period of minutes, with no change in either beam divergence or conversion efficiency. The crystals were mounted in a simple supporting device, and no form of cooling was employed at any time.

Because the 532 nm pump pulse was several orders of magnitude shorter than the upper laser level lifetime, the laser was effectively switched by the extremely rapid development of gain, and a Q-switch was not required to achieve relatively short output pulse widths. YLF is a uniaxial crystal, therefore the wavelength converted output, in both cases, is π polarized with respect to the crystal's c-axis.

In both cases the terminal manifold lifetime is much longer than the driving and output pulse duration. These long lived terminal manifolds impose a restriction of efficiency, in that the laser action will cease when the upper and lower level populations equalize. This

occurs when a fraction, η, (equal to $\beta_u/(\beta_u + \beta_\ell)$ of the ions in the upper level have transitioned to the terminal level, where β_u and β_ℓ are the upper and lower level occupation factors. For Ho:YLF, η is equal to 0.55 and for Er:YLF, η is equal to 0.84.

Other losses in the LDCL oscillator are associated with a fixed threshold and with scattering in the oscillator material itself. Energy must be expended to achieve threshold, and a fraction of the output pulse energy is lost in the cavity due to scattering losses. In addition to scattering, the Ho^{+3} exhibits a slight absorption at 750 nm corresponding to ground state absorption at this wavelength to the $^5I_4$ manifold. This is shown in Figure 15.

9.0 Thulium (Tm^{+3} - $4f^{12}$)

This ion can now be conveniently discussed utilizing both its energy level diagram and also an appreciation for LDCL systems. Laser operation of Tm:YLF at 452 nm when pumped by XeF Rare Gas Halide (RGH) laser, has been reported by J. W. Baer et al.(44). RGH excimer lasers show great promise for operating with overall efficiencies beyond that obtainable in present lamp pumped systems. The XeF RGH laser, operating at 353 nm, resonantly pumps the $^1D_2$ upper state. (See Figure 16.)

Tm:YLF exhibits nearly ideal parameters for high energy laser operation with a value of $\sigma = 3 \times 10^{-20}$ cm^2. This corresponds to a saturation level E_{sat} of approximately 10 joules/cm^2. The $^1D_2$ lifetime, in useful Tm concentrations, is also much greater than the RGH pump pulse duration. Furthermore, in the presence of a saturating optical field, such as in laser operation, most of the initial $^1D_2$ population will undergo purely radiative decay to the $^3F_4$ state, which in turn decays by a spontaneous emission to the ground state. (Please note that the $^3F_4$ state is the lowest excited state of Tm^{+3}. This is the same state which sometimes is referred to erroneously as the $^3H_4$ state.) These advantages are collected in Table IX, which also notes that the energy storage is well below the pump damage limit of such fluoride materials.

Room temperature laser operation of the above state was obtained using an uncoated 5 x 5 x 23 mm crystal of 10% Tm:YLF pumped longitudinally by the XeF laser. With a 2% coupling mirror transmission, threshold was observed at an estimated pump fluence of 4.7 joules/cm^2 at the center of the crystal. Lasing was observed visually as a very intense blue spot, a few meters from the output mirror. The beam divergence was 2.5 milliradians, and the pulse width 45 nanoseconds.

Measurements of the spectroscopic and laser parameters of XeF pumped Tm:YLF have shown the possible loss mechanisms as illustrated in Figure 17. Additionally, this has led to heat load and concentration quenching analysis as shown in Figure 18. The conclusions to date are that the maximum fractional heat load with such material might be as much as 20% which should be coolable through disc cooling technologies.

10.0 Summary

In the above review of the literature associated with crystalline fluoride lasers, we have shown that judicious choice of dopant ion(s), and the expanding availability of both materials and laser pump sources, have greatly opened up the spectral diversity possible for such systems. We expect such developments to continue, associated with the developing of new fluoride host materials, choices of other dopant ions -- both singly and multiply doped, and the availability of still newer pump lasers.

11.0 Acknowledgement

We wish to acknowledge the gracious assistance of Mr. E. P. Chicklis of Sanders Associates, Inc., in providing a large number of the data and figures for this review.

12.0 References

1. L. F. Esterowitz et al. Appl. Phys. Lett. 35 (3) p. 236 (1979).
2. D. J. Ehrlich et al. Optics Letters, 5 (8) p. 339 (1980).
3. E. P. Chicklis et al. "High Power Laser and Materials Investigation" Final Report DoE, Contract DE-AC08-78DP40054.
4. M. Weber, Lawrence Livermore National Laboratory (Private Communication).
5. P. Liu, R. Yen, N. Bloembergen Appl. Optics 18 (7) p. 1015, 1 April 1979.
6. D. J. Ehrlich et al., Optics Lett. 4, p. 184 (1979).
7. D. J. Ehrlich et al., "Tunable UV Solid State Ce:YLF Laser at 325 and 309 nm", Tech. Dig., IEEE/OSA Topical Meering on Excimers, Charleston, S.C. Sept. 11-13, 1979.
8. L. Esterowitz, et al. J. Appl. Phys. 48 (2) p. 650 (1977)
9. C. A. Morrison et al. "Assessment of Pr^{+3}:KY_3F_{10} as a Blue-Green Laser" HDL TR-1897, February 1980.
10. A. L. Harmer, et al., J. Phys. Chem. Solids 30 p. 1483 (1969).
11. E. J. Sharp, et al. J. Appl. Phys. 44, p. 5399 (1973).
12. D. LeGoff et al., Optics Comm. 26 (1) p. 108 (1978).
13. J. Zimmerman, et al., "Oscillators for Phosphate Glass Laser Systems" Topical Meeting on Inertial Confinement Fusion, San Diego, February 1978.
14. S. E. Stokowski, et al. "Fluorophosphate Galss for Fusion Lasers" Topical Meeting on Inertial Confinement Fuison, San Diego, February 1978.
15. J. C. Guyot, Centre de Recherches de la C.G.E. (Private Communication).
16. T. H. Pollak et al., "CW Laser Operation of Nd:YLF" to be published, IEEE J. Quantum Electronics, Feb. 1982.

17. J. Rinefried, U.of Toch., (Private comm.); and N.P.Barnes & D.J.Gettemy, JOSA 70 (10) p.1244 (1980).
18. H. P. Jenssen, et al. J. Q. Electr. 9 p. 665 (1973).
19. T. Y. Fan, S.B. Thesis, MIT (1981) and H. P. Jenssen (private communication) as reported by G. D. Ferguson et al. "Solid State Lasers for Hydrography and Communication" NADC Annual IR/EO Summary, August 1980.
20. M. J. Weber, et al. J. Appl. Phys. 49 (6) p. 3464 (1978).
21. E. P. Chicklis, et al. Appl. Phys. Lett. 19 (4) p. 119 (1971).
22. E. P. Chicklis, et al. IEEE J.Q.E. QE-8 (2) p. 225 (1972).
23. L. F. Johnson, et al. Appl. Phys. Lett. 8 (8) p. 200 (1966).
24. A. M. Morozev, et al., Opt. Spectrosc. 39 (3) p. 338 (1975).
25. I. G. Podkolzinia, et al. Opt. Spectrosc. 40 (1) p. 111 (1976).
26. E. P. Chicklis, et al. IEEE J. Q. E., QE-13 (11) p. 893 (1977).
27. Sh. N. Gifeisman et al. Opt. Spectrosc. 44 (1) p. 68 (1978).
28. D. Gettemy, et al. Rev. Sci. Instr. 54 (9) p. 1194 (1980) and N. P. Barnes, et al. "TEM_{00} Mode Ho:YLF Laser" 1979 LASL Conference on Optics (May 1979).
29. H. P. Jenssen (unpublished results) and quoted in reference (19).
30. A. Linz and R. Eckardt, "2.9μHo:YLF Laser", unpublished results.
31. E. P. Chicklis, et al. Tech. Report ECOM-0013-F (1973) and Final Report Cont. #DAAB07-73-C-0066, March 1974.
32. K. O. White, et al. Appl. Opt. 14, p. 16 (1975).
33. A. Erbil and H. P. Jenssen, Appl. Opt. 19, p. 1729 (1980).
34. V. P. Gapontsev, et al. "Erbium Glass Lasers and their Applications" paper presented at International Conference on Lasers 81, Dec. 14-18, 1981, New Orleans, LA.
35. E. P. Chicklis, et al. "Er:YLF Laser Development" Tech. Report AFAL-TR-75-64 (1975).
36. M. Knights, et al. "1.73 Eyesafe Laser Rangefinder" Sanders Assoc. (Private communication).
37. M. V. Petrov and A. M. Tkachuk, Optics and Spectros. 45 (1) p. 181 (1975).
38. L. Esterowitz, et al. "IR Cascade Solid State Lasers" Proc. of Int'nl. Conf. on Lasers 1979, V. J. Corcoran ed. STS Press, McLean, VA. (1980).
39. E. P. Chicklis, et al. "Two Color Laser Operation in Er-Ho:YLF" Proc. of Tech. Program: Electro-Optics/Laser. 78, Boston, MA. Sept. 19-21 (1978) p. 531.
40. H. W. Gandy and R. J. Ginther, Proc. IRE 50 (10) p. 2114 (1962).
41. P. Moulton (personal communication) and paper presented at Int. Conf. on Lasers '81, Dec. 14-18 (1981) New Orleans, LA.
42. M. G. Knights, et al. Proc. of the Int. Conf. on Lasers '79, V. J. Corcoran Ed. STS Press, McLean, VA. 1980.
43. J. W. Baer, et al. Paper ThA1, Topical Meeting on Excimer Lasers, Sept. 1979.

Figure 1

LASER TRANSITIONS OBSERVED IN YLF

(mostly room temperature)

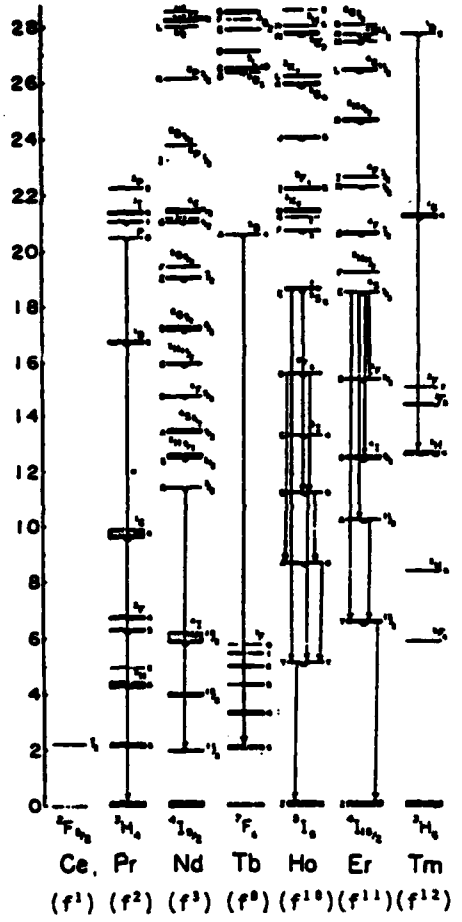

Figure 2

STIMULATED EMISSION CROSS SECTION

Nd:YAG AND Nd:YLF

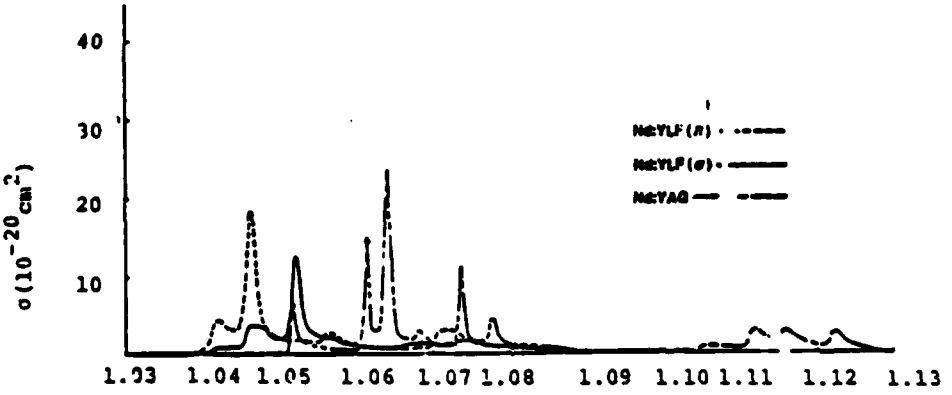

Figure 3

SENSITIZATION PROCESSES IN Ho:αβ:YLF

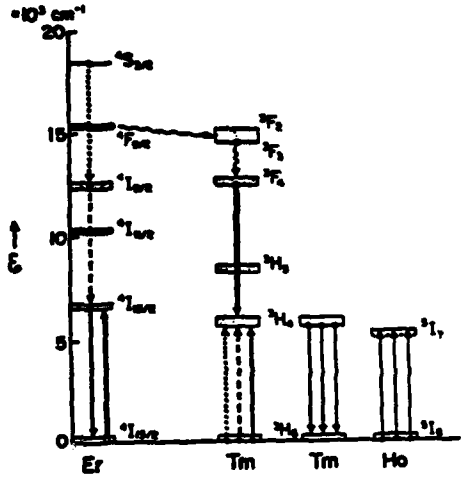

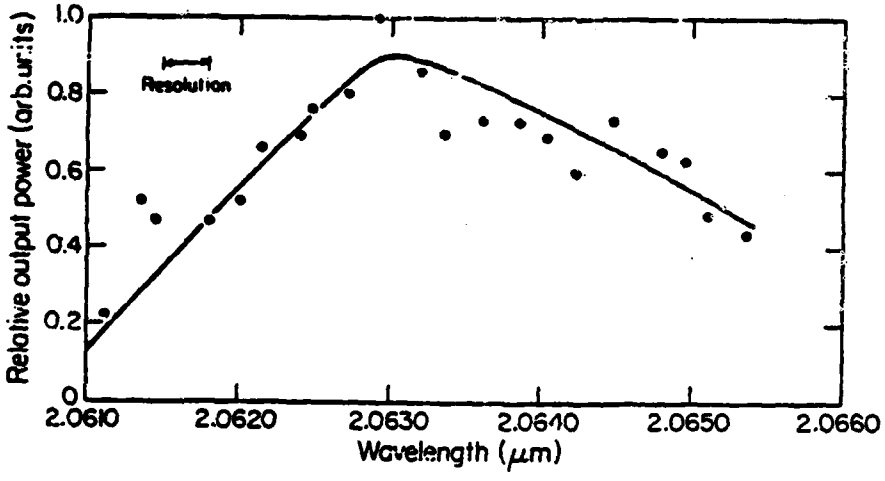

Figure 4

RELATIVE OUTPUT POWER OF THE LASER IN ONE OF THE TUNING REGIONS. THE OTHER REGION OBSERVED WAS FROM 2.0480 TO 2.0559 μm.

Figure 5
POLARIZED EMISSION SPECTRUM OF Ho^{3+}:YLF IN THE WAVELENGTH REGION WHERE TUNABLE LASER OUTPUT WAS OBSERVED.

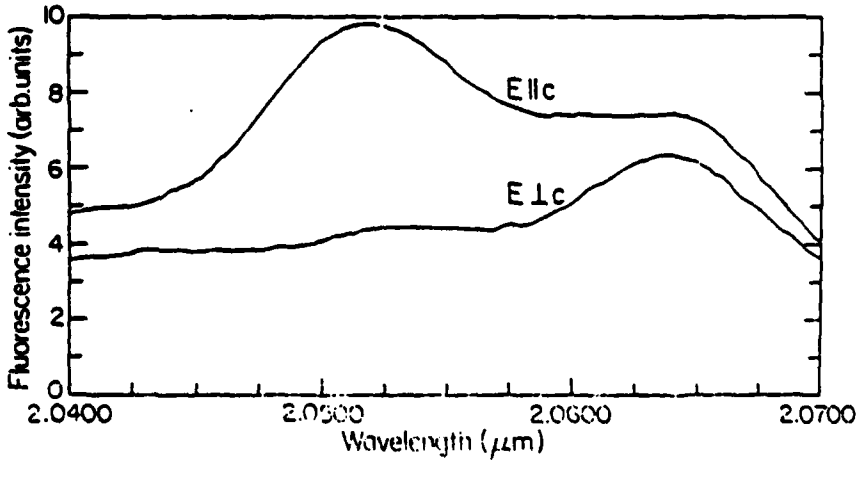

Figure 6
STIMULATED EMISSION CROSS SECTION FOR Ho:αß:YLF

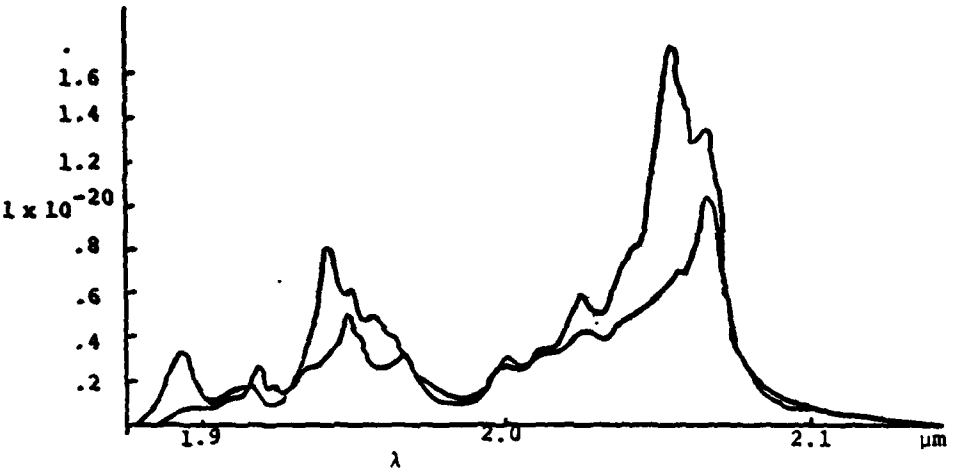

Figure 7
Er:YLF 1.73 μm LASER

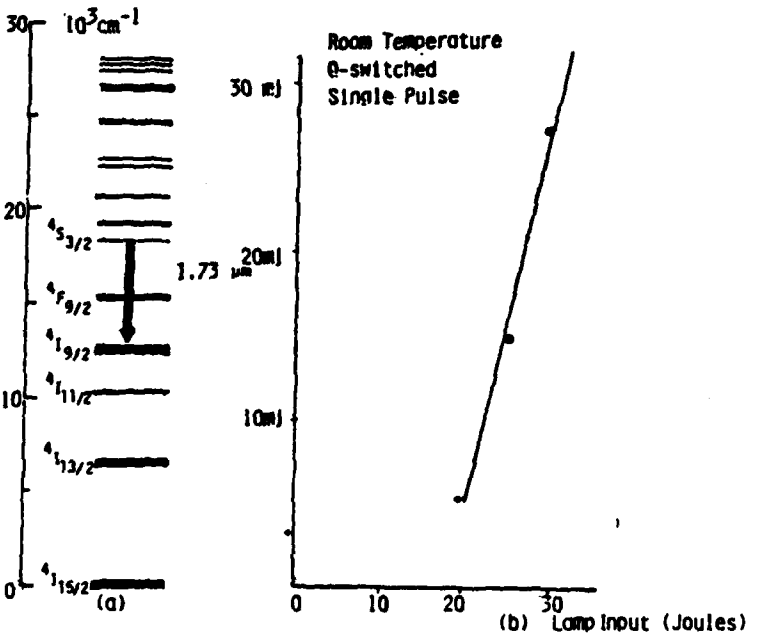

- 4 LEVEL TRANSITION
- RAPID PUMP BAND METASTABLE RELAXATION
- NO ESA, GSA
- LONG UPPER LEVEL LIFETIME

Figure 8

TWO COLOR (0.75/0.85) LASER

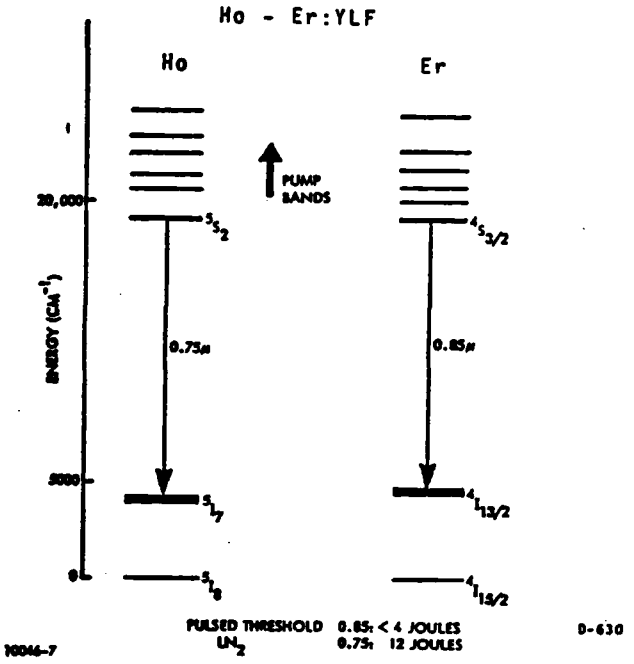

Figure 9

NORMALIZED FLUORESCENCE OF 5% Er, 2% Ho:YLF UNDER SELECTIVE EXCITATION

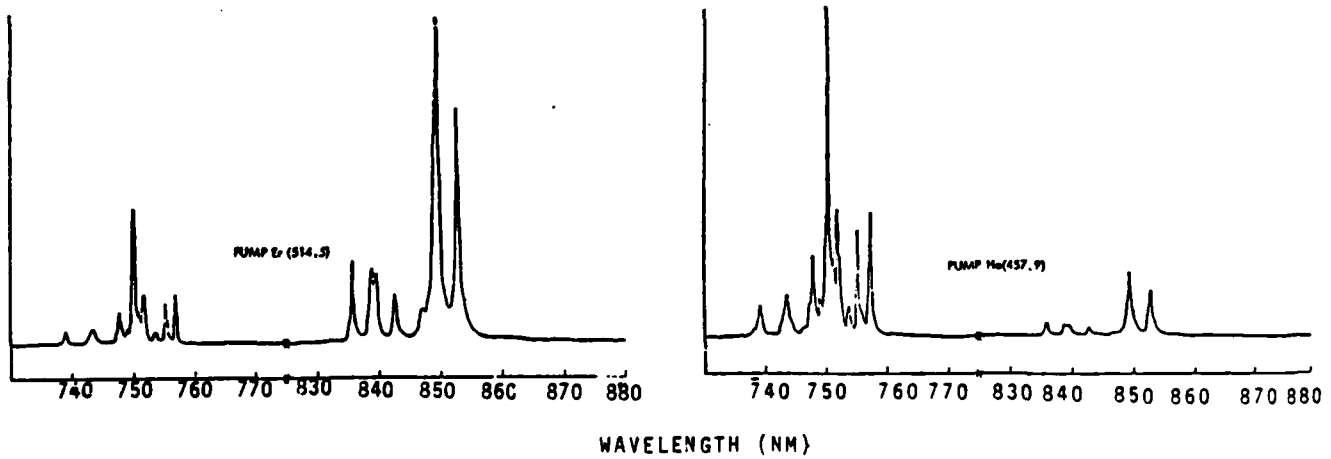

Figure 10

QUENCHING AND TRANSFER RESONANCES
(A: TRANSFER: B,C: QUENCHING)

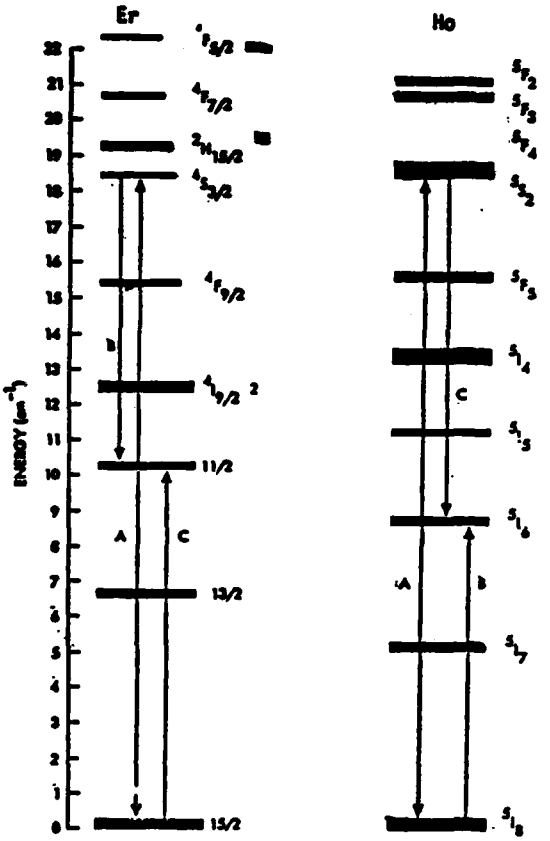

FIGURE 11

0.75/0.85 MICRON LASER PERFORMANCE

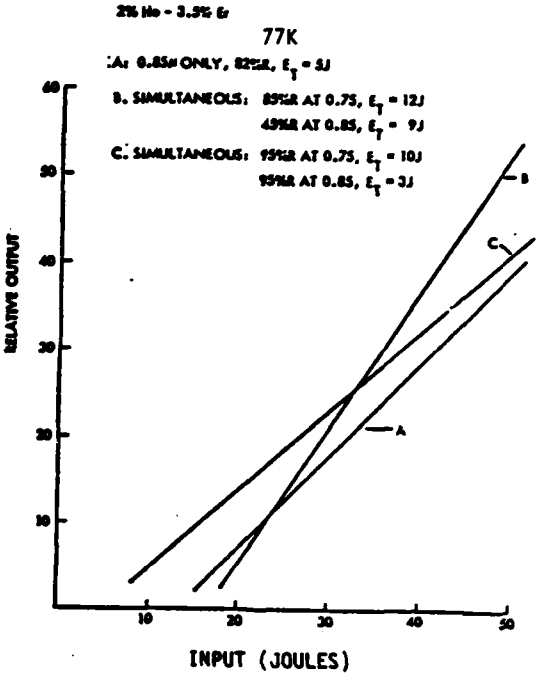

FIGURE 12

IDEAL RESONANTLY PUMPED LASER

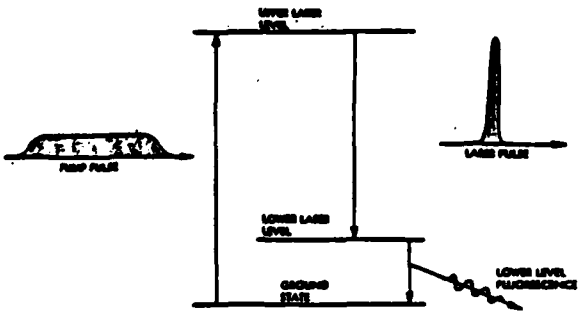

FIGURE 13

532 nm RESONANTLY PUMPED Ho:YLF LASER

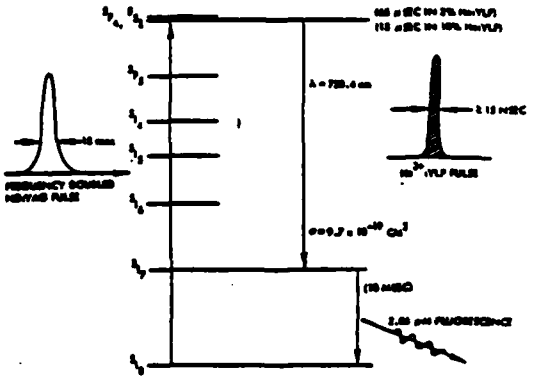

Figure 14

532 nm RESONANTLY PUMPED Er:YLF LASER

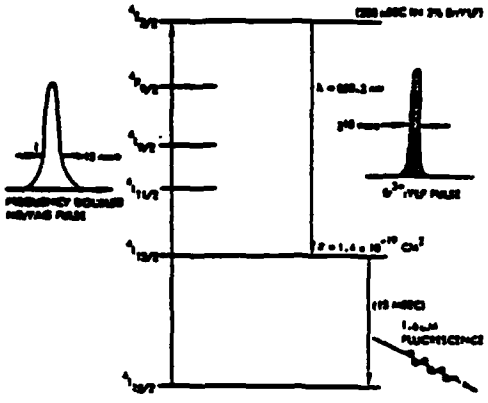

Figure 15

EMISSION AND ABSORPTION SPECTRA OF Ho:$LiYF_4$

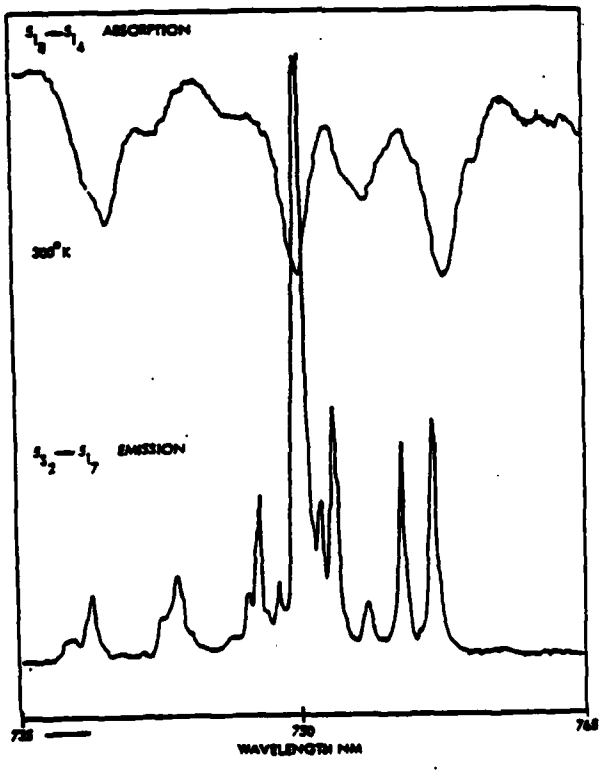

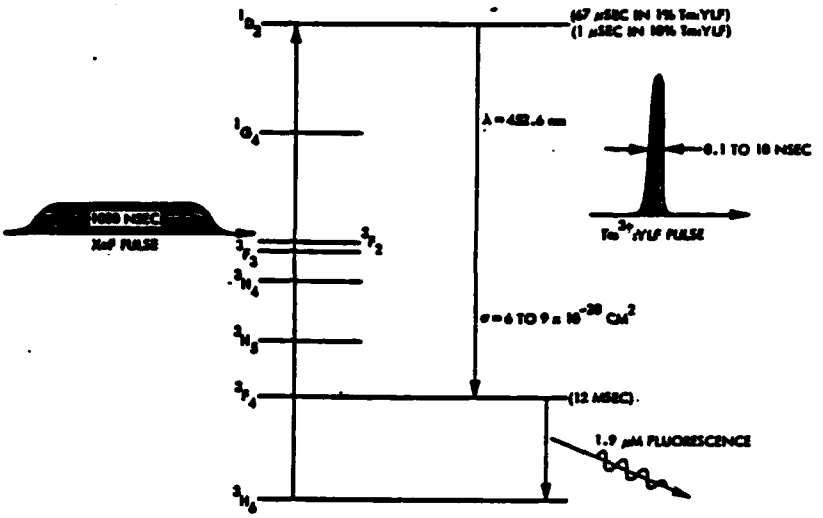

Figure 16
XeF RESONANTLY PUMPED
Tm:YLF LASER

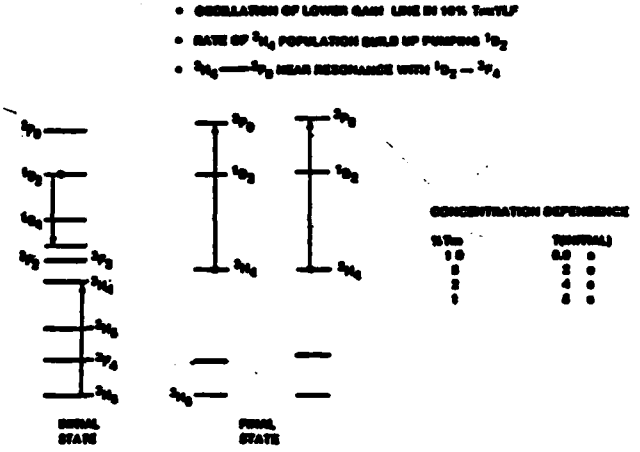

Figure 17
POSSIBLE LOSS MECHANISM IN Tm:YLF

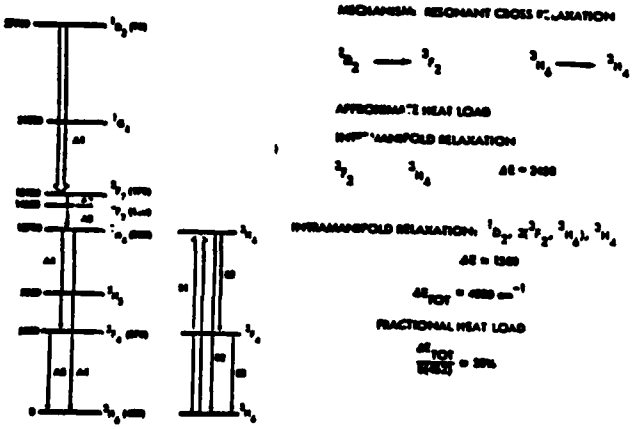

Figure 18
Tm^{3+}:YLF HEAT LOAD ANALYSIS
CONCENTRATION QUENCHING

Table I

Physical Properties of $LiYF_4$ (YLF)

MECHANICAL	YLF
Density (gm/cm^3) (undoped)	3.99
~8%YLF	3.97
Hardness (Mohs)	4-5
Elastic Modulus (N/m^2)	7.5×10^{10}
Poisson's Ratio	0.33
Strength (Modulus of Rupture, in Kg/cm^2)	335
THERMAL	
Thermal Conductivity @ 300°K ($W/cm \cdot °K$)	0.06
Thermal Expansion Coefficient in 0-100° C range -($°K^{-1}$)	a axis : 13.3×10^{-6} c axis : 9.0×10^{-6}
CRYSTALLINE STRUCTURE	Tetragonal (Scheelite)
a - axis (Å)	5.167
c - axis (Å)	10.735
c/a ratio	2.078

Table II

Optical Properties of $LiYF_4$ (YLF)

OPTICAL	
Index of Refraction at λ = 1.06 μm	n_o = 1.4481 n_e = 1.4704
$\frac{\partial n}{\partial T}$ (5° - 50°C) at λ = 1.06 μm	π = -4.3 x 10^{-6} σ = -2.0 x 10^{-6}
Nonlinear Refractive Index n_2 (10^{-13} esu)	0.59 ±0.07
UV Absorption	50% at 0.120 μm
Two Photon Absorption Coefficient β(cm/MW) at λ = 266 nm	<5.0 x 10^{-9}
Damage Resistance (GW/cm^2) at λ = 1.064 μm	>20

Table III

Laser Transitions Observed in YLF (mostly room temperature)

	λ (in nm)	Transition
Ce:YLF	306 to 305 and 323 to 320	$5d \rightarrow 4f\ (^2F_{7/2})$
Pr:YLF	479	$^3P_0 \rightarrow {}^3H_4$
Nd:YLF	1053.0 (σ) 1047.1 (π)	$^4F_{3/2} \rightarrow {}^4I_{11/2}$
Tb:YLF	544.5	$^5D_4 \rightarrow {}^7F_5$
Ho:YLF	749.8	$^5S_2 \rightarrow {}^5I_7$
	1014.3	$^5S_2 \rightarrow {}^5I_6$
	1392. - 1396.	$^5S_2 \rightarrow {}^5I_5$
	979.4	$^5F_5 \rightarrow {}^5I_7$
	1486.	$^5F_5 \rightarrow {}^5I_6$
	2352	$^5F_5 \rightarrow {}^5I_5$
	1673	$^5I_5 \rightarrow {}^5I_7$
	3914	$^5I_5 \rightarrow {}^5I_6$
	2858 - 2952	$^5I_6 \rightarrow {}^5I_7$
	2054 to 2067.2 (Ho:~8%YLF)	$^5I_7 \rightarrow {}^5I_8$
Er:YLF	849 - 855	$^4S_{3/2} \rightarrow {}^4I_{13/2}$
	1210 -1235	$^4S_{3/2} \rightarrow {}^4I_{11/2}$
	1647 -1750	$^4S_{3/2} \rightarrow {}^4I_{9/2}$
	2713 -2870	$^4I_{11/2} \rightarrow {}^4I_{13/2}$
	1530 -1617	$^4I_{13/2} \rightarrow {}^4I_{15/2}$
Tm:YLF	452.6	$^1D_2 \rightarrow {}^3F_4$

Table IV

Comparison of Thermal Properties of Nd Laser Materials

	Nd:YLF	Nd:YAG	Nd:GLASS (Q-98)
THERMAL CONDUCTIVITY at 300°K (w/m-°K)	6.6	11	0.86
THERMAL EXPANSION COEFFICIENT IN 0 to 100°C Range (cm^{-1})	A AXIS 13×10^{-6} C AXIS 8×10^{-6}	7.8×10^{-6}	11×10^{-6}
THERMAL CAPACITY at 300°K (J/C°K)	0.79	0.5	0.88
dN/°T at 1.06 microns	π -4.3 x 10^{-6}* σ -2 x 10^{-6}	7×10^{-6}	-2.9×10^{-6}
THERMAL LENSING**	π>60W σ>150W	>8W	-

*Rinefried - University of Rochester
**J. Murray - Lawrence Livermore Laboratory

Table V

Stimulated Emission Cross Section of Nd:YLF and Nd:YAG

Material	Wavelength	σ
Nd:YLF	~1.047 microns	1.8×10^{-19} cm^2
Nd:YLF	~1.053 microns	1.2×10^{-19} cm^2
Nd:YAG	1.064 microns	2.4×10^{-19} cm^2

Table VI

Properties of KTb_3F_{10} and $LiTbF_4$

	KTb_3F_{10}	$LiTbF_4$
CRYSTALLINE STRUCTURE	CUBIC (FLUORITE)	TETRAGONAL (SCHEELITE)
OPTICAL		
INDEX OF REFRACTION @ λ= 633 nm	1.50	n_e = 1.473 n_o = 1.502
NONLINEAR INDEX n_2 (10^{-13} esu)	~0.7 *	~0.7 *
VERDET CONSTANT V(MIN/Oe-cm) @ λ= 633 nm T = 295°K	0.40*	0.425*
RELATIVE FIGURE OF MERIT** nV/n_2 @ λ =633 nm	4.3 *	4.9 *

*Marvin Weber, Lawrence Livermore Laboratory
**Where Hoya FR-5 is 1

Table VII

Linear Downconversion in Solids Advantages

- Linear process (conventional laser materials)
- Multiwavelength capability
- Metastable lifetime not required for short pump pulse
- Stable medium
- Low thermal loading - uncooled operation

Table VIII

Resonant Pumped Lasers Operating Systems

SYSTEM	λ	PUMP	REMARKS
Tm^{3+}:YLF (SANDERS)	452nm	XeF	RADIATIVE UPPER AND LOWER LEVELS
Er AND Ho:YLF (SANDERS)	850 AND 750nm	532	40 Hz OSCILLATOR DEMONSTRATED USING UNCOOLED CRYSTAL 2% CONVERSION EFFICIENCY
Ho:YLF (NRL)	1.392, 1.673μm 1.392, 3.91μm	535	CASCADE LASER $^5S_2 \rightarrow {}^5I_5 \rightarrow {}^5I_7$ $^5S_2 \rightarrow {}^5I_5 \rightarrow {}^5I_6$
Ni:MgF_2 (LINCOLN)	~1.6—1.7μm	1.06/1.34	IR TUNABLE
Co:MgF_2 (LINCOLN)	~1.6—2.1μm	1.34	IR TUNABLE

Table IX

XeF Pumped Tm^{3+}:YLF

- Tm:YLF exhibits nearly ideal parameters for high energy operation
  $\sigma = 3 \times 10^{-20} cm^2$
  $E_{SAT} \sim 10 J/cm^2$
  $T_f > 10$ s(1% Tm)
- High energy storage well below pump damage limit
  $E_S = 0.6$ J/cm^3 (5 J/cm^2, 2% Tm^{3+})
- Heat load model verified experimentally (DOE)
  10% loading in low Tm concentrations
- Crystal growth scalable to apertures needed for high power system

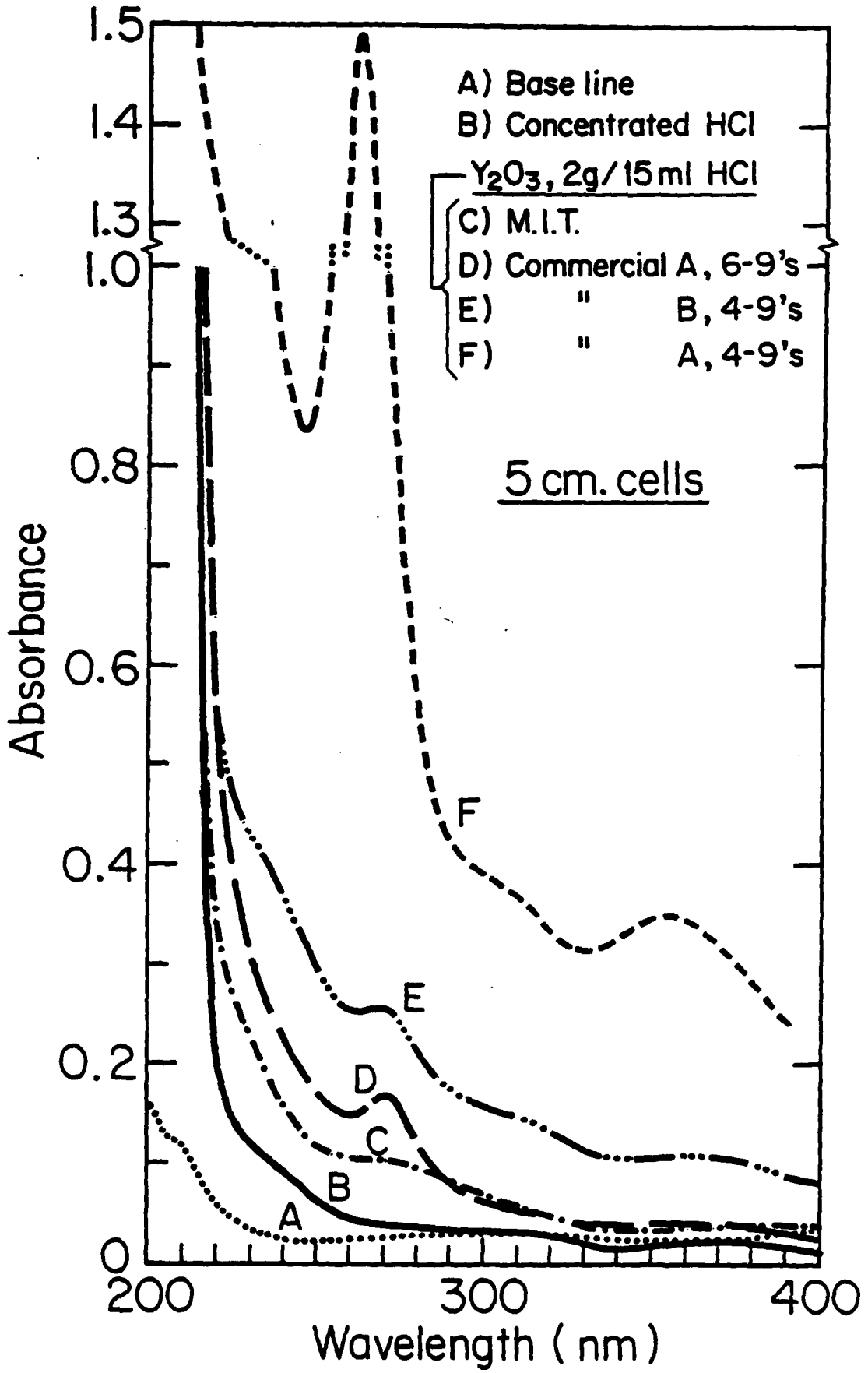
A) Base line
B) Concentrated HCl
Y_2O_3, 2g/15ml HCl
C) M.I.T.
D) Commercial A, 6-9's
E) " B, 4-9's
F) " A, 4-9's
5 cm. cells
Absorbance
1.5
1.4
1.3
1.0
0.8
0.6
0.4
0.2
0
200
300
400
Wavelength (nm)
A
B
C
D
E
F

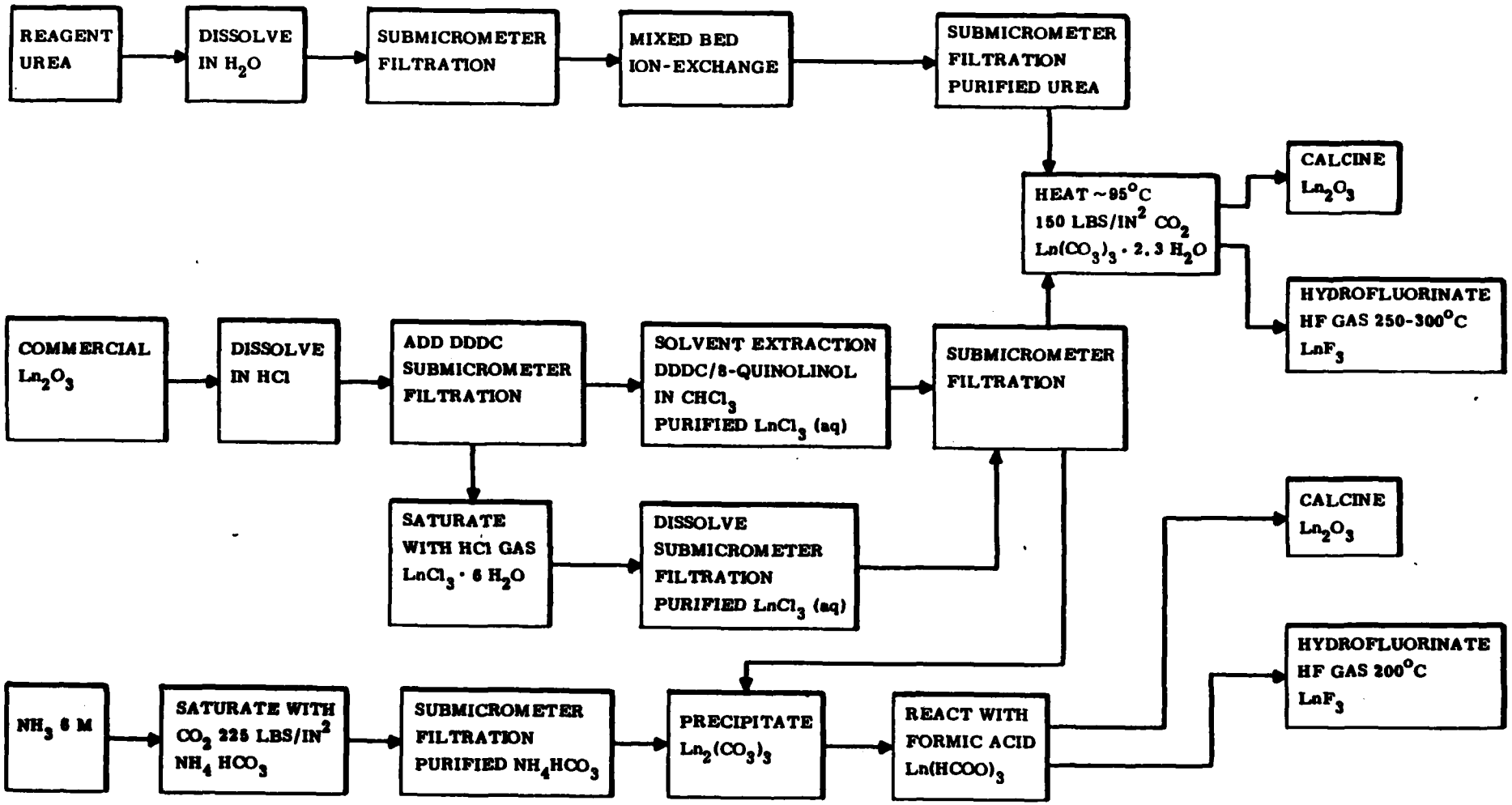

PURIFICATION AND SYNTHESIS OF
RARE EARTH COMPOUNDS

END

FILMED

1-86

DTIC